European Commission

JRC VALIDATED METHODS, REFERENCE METHODS AND MEASUREMENTS REPORT

EU harmonised test procedure: electrochemical impedance spectroscopy for water electrolysis cells

Malkow, T., Pilenga, A., Tsotridis, G.

2018

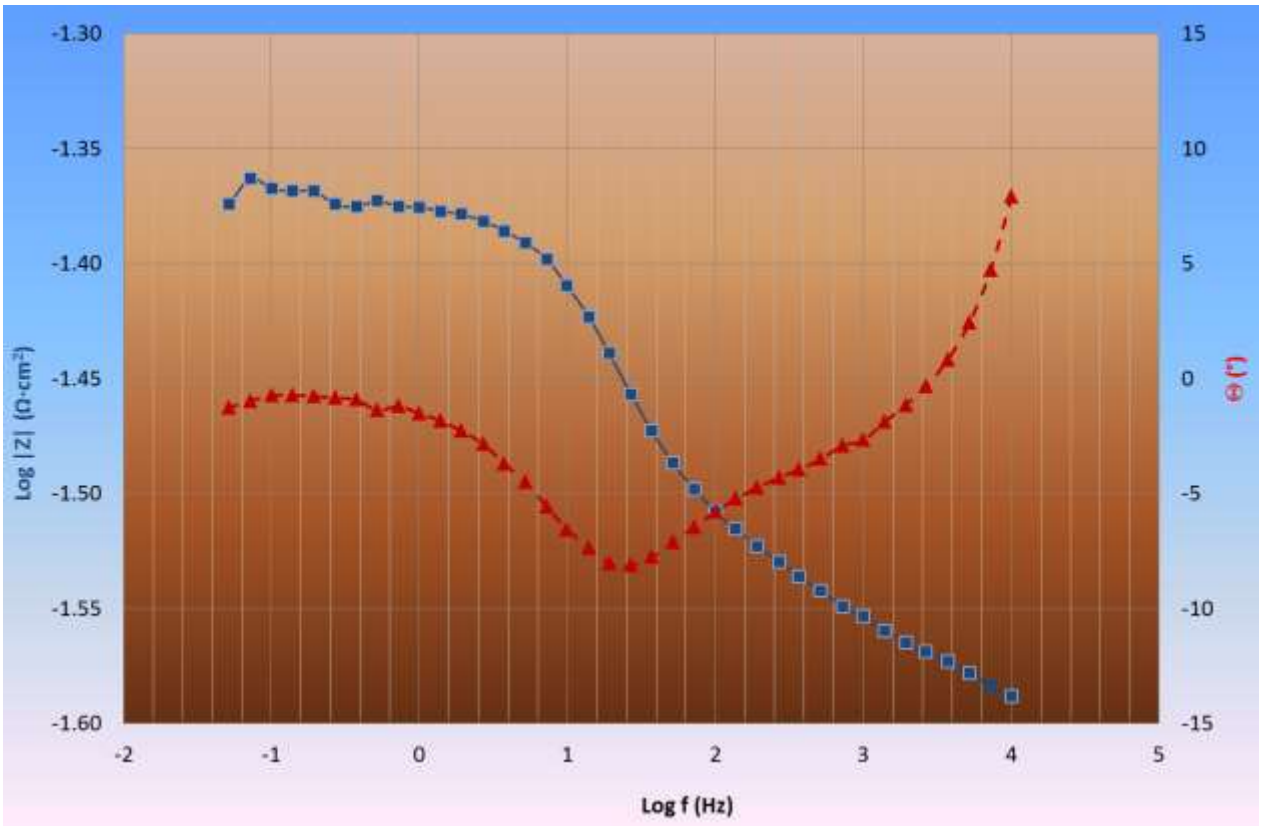

Joint Research Centre

EUR 29267 EN

This publication is a Validated Methods, Reference Methods and Measurements report by the Joint Research Centre (JRC), the European Commission's science and knowledge service. It aims to provide evidence-based scientific support to the European policymaking process. The scientific output expressed does not imply a policy position of the European Commission. Neither the European Commission nor any person acting on behalf of the Commission is responsible for the use that might be made of this publication.

Contact information
Name: Thomas MALKOW
Address: European Commission, Joint Research Centre, Westerduinweg 3, 1755 LE Petten, The Netherlands
Email: Thomas.Malkow@ec.europa.eu
Tel.: +31 224565122

JRC Science Hub
https://ec.europa.eu/jrc

JRC107053

EUR 29267 EN

Print	ISBN 978-92-79-88738-3	ISSN 1018-5593	doi: 10.2760/67321
PDF	ISBN 978-92-79-88739-0	ISSN 1831-9424	doi: 10.2760/8984

Luxembourg: Publications Office of the European Union, 2018

How to cite this report: T. Malkow, A. Pilenga, G. Tsotridis, *EU harmonised test procedure: electrochemical impedance spectroscopy for water electrolysis cells*, EUR 29267 EN, Publications Office of the European Union, Luxembourg, 2018, ISBN 978-92-79-88738-3, doi: 10.2760/67321, JRC107053

Printed in the Netherlands

EU harmonised test procedure: electrochemical impedance spectroscopy for water electrolysis cells

Malkow, T., Pilenga, A., Tsotridis, G.

Contents

Foreword

This report was carried out under the Framework Contract between the Joint Research Centre (JRC) and the Fuel Cells and Hydrogen 2 Joint Undertaking (FCH2JU) implemented by annual Rolling Plans.

In accordance with the 2018 rolling plan, this report was prepared under this contract as the part relating to the "Testing procedures" of deliverable B.2.3 "Harmonised Electrolysis Testing".

THIS PAGE IS LEFT BLANK INTENTIONALLY

Acknowledgements

We would like to express our sincere gratitude to all participants and their respective organisations for their contributions to developing the EU harmonised test procedure on electrochemical impedance spectroscopy for electrolysis cells document for low temperature water electrolysis applications.

We would also like to thank the FCH2JU Programme Office, and in particular Dr. Nikolaos Lymperopoulos, for the continuous support and encouragement we received throughout the preparatory stages of this report. The FCH2JU is also thanked for its financial contribution.

THIS PAGE IS LEFT BLANK INTENTIONALLY

List of contributors

(in alphabetical order of their organisations and names)

AREVA H_2Gen	AREVA H_2Gen	Fabien Auprêtre
Deutsches Zentrum für Luft- und Raumfahrt German Aerospace Center	Deutsches Zentrum für Luft- und Raumfahrt e. V.	Regine Reißner
Empa Materials Science and Technology	Swiss Federal Laboratories for Materials Science and Technology	Ulrich Vogt
Université Paris Sud	Institut de Chimie Moléculaire et des Matériaux d'Orsay – Université Paris-Sud	Pierre Millet
Consiglio Nazionale delle Ricerche / ITAE	Istituto di Tecnologie Avanzate per L'Energia "Nicola Giordano"	Antonino S. Aricó

THIS PAGE IS LEFT BLANK INTENTIONALLY

1. Introduction

Electrochemical impedance spectroscopy (EIS) is a suitable and powerful diagnostic method for polymer electrolyte membrane water electrolysis cells (PEMWE), anion-exchange membrane water electrolysis cells (AEMWE) and alkaline electrolysis cells (AWE) because it is non-destructive and provides useful information *in-operando* on performance and cell voltage losses associated with particular components.

EIS measures the frequency dependence of the impedance, Z, of a water electrolysis (WE) cell by applying a small alternating current (AC) in galvanostatic mode as a perturbation signal while measuring the alternating cell-voltage response.

In potentiostatic mode, a small alternating voltage is applied and the AC response is measured. The use of small (sinusoidal) signals assumes negligible harmonic content in the recorded response.

A broad frequency range over several decades will enable identification of the electrochemical and transport processes (e.g. double layer charging, charge transfer, interfacial capacitance, gas diffusion) taking place in the WE cell over a range of different time scales (i.e. 10^{-6} to 10^{3} s).

The choice of the limits of the frequency range, and in particular its population, requires that the anticipated total measurement time is accounted for in order not to compromise the stability of the data measured when the cell is operated.

Particularly in PEMWE cells and AEMWE cells, EIS is principally used to optimise the structure of membrane electrode assemblies (MEAs) and to quantify changes in the parameters of the elements representative of the cell components in an electrical equivalent circuit (EEC) model to simulate cell impedance.

Analysis by fitting EEC models to the impedance data obtained under different operating conditions facilitates determination of the contributions of the different physicochemical processes to the overall WE cell impedance in different conditions.

The main contributions to losses in WE performance (cell-voltage losses) are due to:

- ohmic resistance, R_{Ω}, associated with proton and electron conduction in the MEA, current collector and flow plates and
- electrode kinetics at the electrode/electrolyte interfaces and mass transport of reactant gases resulting collectively in the polarisation resistance, R_p.

The reaction kinetics could be improved by using advanced catalysts and forming appropriate catalyst/electrolyte interfaces.

Ohmic losses could be reduced by decreasing the hindrance on proton and electron movements within the membrane electrolyte, electrodes, monopolar/flow field plates, current collectors and their respective interfaces.

Therefore, EIS measurements in WE cell performance characterisation studies aim to:

- Identify individual contributions to the total WE cell impedance particularly R_{Ω} and R_p.
- Estimate other electrochemical parameters (double layer capacitance, C_{dl}, charge transfer resistance, R_{ct}, adsorption resistance, R_{ad}, adsorption inductance, L_{ad}, etc) by

complex non-linear least square (CNLS) analysis of an appropriate EEC model to simulate the measured impedance of the WE cell test set-up.

- Provide information that could assist in optimising WE cell components and operating conditions.

The user of this method should also refer to the extensive scientific literature on EIS [1-4].

2. Objective and scope

This procedure is a general electrochemical characterisation method that is used in the research into and development of WE single cells. The test can be used as a baseline measurement for the qualification of the performance of a WE cell and its components for a given application.

The aim of the EIS measurements is to record frequency spectra at steady state, from which the impedance is determined as a function of the perturbation frequency in order to discern the various contributions of the electrochemical and transport processes to the polarisation of the WE cell.

This procedure is primarily addressed at those performing EIS measurements on WE single cells. It describes the measurement methodology and provides a graphical presentation of the recorded data. It also recommends data validation and analysis methods.

The user should also refer to the scientific literature for additional, more in-depth analysis.

THIS PAGE IS LEFT BLANK INTENTIONALLY

3. Terminology, definitions, and symbols

3.1. Terminology and definitions

Galvanostatic/potentiostatic EIS measurement

A galvanostatic EIS measurement is characterised by an AC perturbation signal applied to the operating WE cell.

A potentiostatic EIS measurement is characterised by an alternating voltage perturbation signal imposed on the operating WE cell.

Frequency response analyser

A frequency response analyser (FRA) measures the gain and phase response characteristics with respect to the frequency of the device or system under test, by applying a frequency-swept voltage or current sine wave and examining its response signal.

Sensor

A sensor is a device that measures a physical quantity and converts it into a signal that is transferred to a data-acquisition system. Each sensor (including the complete measurement chain) has a specific measurement uncertainty.

Causality

The response of the WE cell test set-up must be entirely determined by the applied perturbation. The output depends only on the present and past input values.

Linearity

The WE cell test set-up is linear when its response to a sum of individual input signals is equal to the sum of the individual responses. For linear systems the response is independent of the amplitude.

Stability

The WE cell test set-up should return to its original state once the perturbation is removed.

Measurement electrode

A measurement electrode (Working, Counter, Reference/Sense 1 and Reference/Sense 2) in the test set-up is an electrical conductor (current collector) used to make contact between a WE cell and the potentiostat/galvanostat and/or the FRA. These connections are made through shielded cables.

Test bench

A test bench consists of a set of sensors, actuators, control loops, piping, data-acquisition systems, etc. that allows operation and testing of a single cell. The DC power supply is generally integrated into the test bench.

More extensive terminology definitions can be found in [8-11].

3.2. Symbols

The symbols used in this document are defined as follows:

Table 1. Definition of symbols

Symbol	Description (unit)
A	Geometric electrode* area (m^2)
$_{ACS}$	Subscript referring to AC signal sampling (-)
$_{ACT}$	Subscript referring to AC signal response (-)
α	Arbitrary power exponent (-)
C	Capacitance (F or $F.cm^{-2}$)
C_{CPE} (Q_C)	Pseudo-capacitance (Q_C) ** of a capacitive constant phase element (CPE) approximating the capacitance of the double layer of a WE cell electrode accounting for the fractal and porous nature of the electrode including roughness ($F.s^{-\alpha}$ or $F.s^{-\alpha}.cm^{-2}$)
C_{dl}	Capacitance of the double layer of a WE cell electrode (F or $F.cm^{-2}$)
d	Thickness of the GDE (m)
e	Electron charge, 1.602×10^{-19} (C or $F.cm^{-2}$)
F	Faraday's constant, 96,485 ($C.mol^{-1}$)
f	Perturbation frequency in EIS (Hz)
f_{HI}	High limit of perturbation frequency (Hz)
f_{LOW}	Low limit of perturbation frequency (Hz)
i	Imaginary unit with property $(\pm i)^2 = -1$ (-)
i_0	Exchange current density ($A.cm^{-2}$)
$I_{AC,\,k}\,(f)$	Galvanostatic method: constant amplitude of AC at *f* (A) Potentiostatic method: AC part of the total current response at *f* (A)

Symbol	Description (unit)
$I_{DC,\,k}$	Direct current (DC) supplied (A)
k	Index to signify the kth steady state of the WE cell where EIS spectra are to be recorded (e.g. at a given direct current (DC) or cell voltage)
k_B	Boltzmann constant, 1.38 × 10^{-23} (J.K^{-1})
L	Inductance (H)
L_{ad}	Inductance associated with the resistance R_{ad} due to species adsorption / desorption at the catalyst surface of a WE cell electrode (H)
L_c	Inductance due the cables/wires used in the WE cell test set-up (H)
N_A	Avogadro's constant, 6.02 × 10^{-23} (mol^{-1})
n_e	Number of electrons exchanged in the cell reaction (-)
$n_{k,\,ACS}$	Number of perturbation cycles at f performed during $\tau_{ACT}(f)$ (-)
$n_{k,\,ACT}$	Number of perturbation cycles at f performed during $\tau_{ACS}(f)$ (-)
$\theta_k(f)$	Impedance phase (principal argument) at f (°)
PPD	Number of frequency data points per decade of frequency range in EIS (-)
Q_C	Pseudo-capacitance of a capacitive CPE (F.s$^{-\alpha}$ or F.s$^{-\alpha}$.cm^{-2}) **
Q_L	Pseudo-inductance of an inductive CPE (H.s$^{\alpha}$ or H.s$^{\alpha}$.cm^{-2}) **
Q_R	Pseudo-capacitance of a resistive CPE (Ω.s$^{\alpha}$ or Ω.s$^{\alpha}$.cm^{-2}) **
R	Resistance (Ω or Ω.cm^2)
R_{ad}	Resistance associated with the inductance L_{ad} due to species adsorption/desorption at the catalyst surface of a WE cell electrode (Ω or Ω.cm^2)
R_{ct}	Resistance due to charge transfer at a WE cell electrode (Ω or Ω.cm^2)
R_Ω	Ohmic resistance estimated at f_{HI} for $\lim_{\lvert f\rvert\to f_{HI}} Z_{IM} = 0$ in a Nyquist plot (high frequency intercept on the real axis) or $\lim_{\lvert f\rvert\to f_{HI}} \theta(f) = 0$ in a Bode plot (Ω or Ω.cm^2)
R_p	Polarisation resistance estimated at f_{LOW} for $\lim_{\lvert f\rvert\to f_{LOW}} Z_{IM} = 0$ in a Nyquist plot (low frequency intercept on the real axis) or $\lim_{\lvert f\rvert\to f_{LOW}} \theta(f) = 0$ in a Bode plot (Ω or Ω.cm^2) as the difference of the total measured resistance (real part impedance) to R_Ω (Ω or Ω.cm^2)
T	Absolute temperature of the WE cell (K)

Symbol	Description (unit)
$U_{AC,k}(f)$	Galvanostatic method: alternating part of the total voltage response at *f* (V) Potentiostatic method: constant amplitude of alternating perturbation voltage at *f* (V)
U_T	Thermal voltage (V)
Y	Measured (potentiostatic perturbation) or calculated (galvanostatic perturbation) WE cell admittance (S or S.cm^{-2})
Z	Measured (galvanostatic perturbation) or calculated (potentiostatic perturbation) WE cell impedance (Ω or Ω.cm^2)
Z^*	Complex conjugate of the measured WE cell impedance (Ω or Ω.cm^2)
Z_D	Diffusion impedance representing a distributed element in an EEC model (Ω or Ω.cm^2)
$Z_{IM,k}(f)$	Imaginary part of impedance (reactance) at *f* (Ω or Ω.cm^2)
$Z_{RE,k}(f)$	Real part of impedance (resistance) at *f* (Ω or Ω.cm^2)
$\|Z_k\|(f)$	Impedance magnitude at *f* (Ω or Ω.cm^2)
ε_o	Permittivity of vacuum (free space), 8.85×10^{-12} (F.mol^{-1})
ε_r	Dielectric constant (relative electrical permittivity) of the GDE (-)
τ	Time constant of an EEC model (s)
$\tau_{ACS}(f)$	Signal sampling time at *f* to perform the specified number of perturbation cycles, n_{ACS} (s) including recording of frequency spectra (s)
$\tau_{ACT}(f)$	Transient response time at *f* to perform the specified number of perturbation cycles, n_{ACT} without recording frequency spectra (s)
τ^a	Time constant for the WE cell anode due to C_{dl} in parallel with R_{ct} (s)
τ_{ad}	Time constant for adsorption/desorption at the WE anode due to L_{ad} in series with R_{ad} (s)
τ^c	Time constant for the WE cell cathode due to C_{dl} in parallel with R_{ct} (s)
τ_D	Time constant for the WE cell cathode due to C_{CPE} in parallel with Z_D (s)
τ_Ω	Time constant for a WE cell test set-up due to L_c in series with R_Ω (s)
$\omega = 2\pi f$	Angular perturbation frequency (Hz)

(*) The electrode is sometimes referred to as gas diffusion electrode (GDE).

(**) The admittance of a capacitive CPE, an inductive CPE and resistive CPE has dimension H.s$^{\alpha}$ or H.s$^{\alpha}$.cm^2, F.s$^{-\alpha}$ or F.s$^{-\alpha}$.cm^2 and S.s$^{-\alpha}$ or S.s$^{-\alpha}$.cm^{-2}, respectively.

4. Test equipment and set-up

A comprehensive EIS experiment requires a combination of equipment:

- Potentiostat/Galvanostat instrument or electronic load bank capable of amplifying AC signals to the required magnitude;
- Sine waveform generator and AC voltage/current waveform analyser (at least one single channel to measure impedance at a time) - usually, both are combined in an FRA;
- DC power supply directly connected to the WE cell anode and cathode and properly sized in terms of current and power.

Note that an alternative to the use of an FRA is to use high frequency sampling (at a level of at least twice the maximum perturbation frequency) followed by fast Fourier transformation (FFT) on both the (sinusoidal) signal and the response signal to obtain discrete frequency spectra via subtraction of the DC contribution.

The ratio (complex valued proportionality factor) of the fundamentals of the frequency spectra of the response (output) and that of the perturbation (input) is the sought impedance,

$$Z(f) = \frac{U_{AC}(f)}{I_{AC}(f)} = |Z(f)| \cdot e^{i\theta(f)} \quad (1)$$

in a galvanostatic EIS measurement while it is the admittance (inverse of impedance),

$$Y(f) = Z^{-1}(f) = \frac{I_{AC}(f)}{U_{AC}(f)} = |Z(f)|^{-1} \cdot e^{-i\theta(f)} \quad (2)$$

for a potentiostatic EIS measurement.

It is commonly assumed that the contributions from any harmonic of the perturbation frequency are sufficiently small in amplitude to be negligible. This presumption may be readily verified using an oscilloscope.

EIS measurement is preferably performed by a classic four electrode measurement configuration with a working electrode, a counter electrode and two reference / sense electrodes.

In some configurations each reference electrode is connected to respectively the working electrode and the counter electrode (two wire configuration).

The test set-up should be connected in such a way as to avoid measuring parasitic current flowing into the load, which affects the measurement as otherwise artefacts may appear at high frequency in the impedance plots.

The voltage response of the WE, U_{AC} is measured across it.

The appropriate shunt for the EIS measurement equipment should be selected according to a compromise between two mutually opposing effects: (a) it should be as small as possible to minimise generation of Joule heat in the shunt and (b) it should be large enough for the voltage drop across it to satisfy the range and the resolution requirements of the respective AC analyser input.

The immediate vicinity of the entire test set-up should be free of electromagnetic sources to avoid interference with the EIS measurement.

Also, a good practice is to use low-inductance cables, i.e. they should be shielded, twisted around each other and as short as possible. In addition, the cross sections of the counter and working electrodes should be as large as possible.

Prior to an EIS measurement, the test set-up can be evaluated when the cell is substituted with a model (dummy) circuit made up of known elements, for example, resistors and capacitors, to determine the accuracy and resolution of the EIS measurement device.

5. Test inputs and test outputs

The test input is a physical quantity that defines the test conditions.

Two types of test input are described below: static input parameters, which are kept constant during EIS measurement and variable input parameters, i.e. those that are varied during EIS measurement.

5.1. Static test inputs

Static inputs do not vary during the entire duration of the test and depend on the MEA used.

Static inputs for the galvanostatic EIS measurement and potentiostatic EIS measurement are given in Table 2.

Table 2. Static input parameters and settings for the EIS instrument

	Test input	Symbol	Unit	Recommended value / range
	Number of perturbation frequency data per decade of frequency range	*PPD*	-	minimum 3
	Number of perturbation cycles during τ_{ACT} (τ_{ACT} *precedes* τ_{ACS})	n_{ACT}	-	minimum 2 (*)
	Number of perturbation cycles during τ_{ACS} *used to record the* EIS spectra (τ_{ACS} *follows* τ_{ACT})	n_{ACS}	-	minimum 3
	Range of perturbation frequencies	f	Hz	10^{-2}–10^{+6}
Potentiostatic method	load (voltage) perturbation peak-to-peak amplitude	U_{AC}	V	typically 5-10 mV_{rms} to be less than the thermal voltage, U_T (e.g. <30 mV at 80°C cell temperature) (†)
Galvanostatic method	load (current) perturbation peak-to-peak amplitude	I_{AC}	A	0.5% – 5% of I_{DC} (‡)

(*) The average of the recorded data is compared to a single cycle or a small number of cycles more likely to represent the true impedance for a large number of identical repetitive perturbation cycles as random noise is

minimised by averaging. This is at the expense of an extended measurement period that would carry the risk of the cell drifting to another state during the measurement, thereby invalidating the data recorded.

(†) Thermal voltage, $U_T=k_BT/e$.

(‡) Subjected to linearity verification, see Sec 6.2 below.

Note that a voltage perturbation below the thermal voltage is required to obey linearity. In the linear regime it is immaterial whether the EIS measurement is performed in galvanostatic or potentiostatic mode [1].

However, too low a perturbation amplitude will result in an unacceptable signal-to-noise ratio, making it difficult for the FRA to distinguish between the actual response and the noise arising from random excitations.

Note that time-domain noise shows up in the response signal after Fourier transformation to the frequency domain, thereby affecting the impedance measurement.

In addition, the continuous regulation of reactant flow and pressure by the controls of the test stand result in fluctuations of these quantities, and ultimately in the WE cell output, whether cell voltage or current. These fluctuations are additional sources of excitation that also affect the measured impedance.

An oscilloscope could be used to identify and quantify both the noise level of electromagnetic radiation noise level in the vicinity of the tested WE cell and the fluctuations arising from regulation by the controls of the test bench.

As a matter of good practice a root mean square (rms) AC voltage of 10 mV_{rms} is recommended as the sinusoidal perturbation in potentiostatic EIS measurements.

5.2. Variable test inputs

The variable test inputs are those physical drivers that influence the test object's behaviour and are changed in a user-programmable manner during a single experiment through the use of suitable control equipment.

The main variable input parameter for EIS is the AC signal perturbation frequency, *f*, controlled by the AC generator.

There are two other variable inputs: the AC signal sampling time, τ_{ACS}, to record the EIS data and the preceding AC response time, τ_{ACT}, accounting for the decay of the previous perturbation signal.

These input variables are controlled by the AC analyser, where τ_{ACS} is always linked to *f*.

Table 3 gives the details of these two variable inputs, including recommended values/ranges and measurement uncertainties.

Table 3. Variable test input parameters for the EIS measurement

Input	Recommended value / range	Measurement uncertainty
$\tau_{ACS}(f)$	time required to perform the specified number of perturbation cycles	±1%

$\tau_{ACT}(f)$	time required to perform the specified number of perturbation cycles	±1%

5.3. Test outputs

The primary test output parameters are the measurable physical quantities that constitute the response of the WE single cell. Table 4 provides details of them.

Table 4. Test output parameters for the EIS measurement

Output	Parameter type	Measurement uncertainty	Sampling rate	
$U_{AC,k}(f)$	primary	± 1%	≥ 20 ($\tau_{ACS}(f)/\tau_{ACT}(f)$)	Galvanostatic method
$I_{AC,k}(f)$	primary	± 1%	≥ 20 ($\tau_{ACS}(f)/\tau_{ACT}(f)$)	Potentiostatic method
$Z_{IM,k}(f)$	secondary	– (*)	–	Nyquist plot (†)
$Z_{RE,k}(f)$	secondary	– (*)	–	Nyquist plot (†)
$\|Z_k\|(f)$	secondary	– (*)	–	Bode plot (‡)
$\theta_k(f)$	secondary	– (*)	–	Bode plot (‡)

(*) Calculated according to the GUM Guide [9] from U_{AC} and I_{AC}

(†) Two dimensional plot of negative imaginary part impedance vs. real part impedance

(‡) Two dimensional plot of impedance magnitude and phase vs. (logarithmic) frequency

THIS PAGE IS LEFT BLANK INTENTIONALLY

6. Test procedure

6.1. Procedure

For the EIS measurement, whether galvanostatic or potentiostatic, the following recommendations apply.

- Make proper (working, counter and reference) electrode connections.
- Set and monitor the test conditions including DC current and voltage.
- When a steady state is reached, set AC or voltage amplitude and monitor all DC and AC parameters to record any deviation from a steady state (stability).
- Set the EIS frequency range.
- Perform linearity verification starting with low perturbation amplitude (see Section 6.2).
- Choose an appropriate number of data points to be recorded per decade of the perturbation frequency range (see Table 2).
- Perform a series of AC perturbations at discrete frequencies, *f*, from a defined range of low to high frequency (or vice versa) with the same sampling governed by the *PPD* parameter (see Table 2). It is recommended that the measurement be carried out from high to low frequencies, making it possible for an experienced practitioner to quickly ascertain whether the measurement is giving reasonable results. It also ensures that a sufficient number of valid data points are recorded for use in a subsequent analysis when it is determined that a cell has drifted to another state during the measurement.

6.2. Data validation

It is recommended that the recorded raw EIS data be subjected to a consistency check to eliminate rogue data (outliers, wild points, recorded data coinciding with the electric grid frequency and harmonics) and that the validity of the recorded EIS data be verified [13-15].

EIS data should satisfy the main principles of linear time-invariant (LTI) systems: **causality** (no effect before its cause), **linearity** (superposition) and **stability** (time invariance), in addition to continuity (no discontinuities) and boundedness (finite impedance) at all frequencies, including at zero and infinity [1,3]. For this reason, the data should be subjected to a numerical validation based on the Kramers-Kronig (KK) integral transform relations [16,17] for the interrelated real and imaginary parts of the impedance. Invalid data should consequently be rejected as not suitable for further analysis.

This approach might necessitate test repetition with improved control of the test conditions and proper selection of parameters, along with comprehensive identification of all potential sources of noise in the vicinity of the test set-up, including the measurement equipment.

EIS data obeying the KK relations within acceptable numerical and experimental error ranges ([1]) (see Table 4) are presumed valid experimental data compliant with the said LTI principles [18,19].

At a given steady state (DC or voltage), **causality** in an EIS measurement should in principle be verified experimentally by measuring zero response except noise, or measuring a response that rapidly decays to the noise level as soon as the perturbation is switched off.

([1]) The numerical error will depend on the numerical estimation method employed while the experimental error will depend on the instrument uncertainty and the measurement uncertainty.

Linearity [7] may be experimentally verified by applying a multiple (fraction) of the selected AC signal to record the same multiple (fraction) in response, i.e. the recorded EIS spectra should coincide within acceptable error ranges.

Stability [1,3] may be experimentally verified either by performing the same experiment through repetitive application of the same input to measure each time within acceptable error ranges the same output each time, or by sweeping frequencies back and forth.

For example, an insignificant hysteresis in the response should be observed when sweeping (a) from high frequency to low frequency and then (b) from low frequency to high frequency as the EIS spectra should coincide within acceptable error ranges.

Compromised stability in an EIS measurement of a WE cell is also exhibited by a considerable change (drift) in the DC value of the current when the potentiostatic method is applied and in the cell voltage when the galvanostatic method is applied.

The impedances of a WE cell test set-up exhibit capacitive and/or inductive storage losses and dissipation (resistance) losses.

By the very nature of EIS measurements, these impedances are measured generally with **finite** (bounded) magnitude at discrete frequencies within a set range. It makes it impossible to know of any impedance unboundedness outside the measured range of frequencies.

Within this range, impedance singularities (discontinuities) are unfortunately in most cases also not directly detectable experimentally.

This is unless the perturbation frequency is at or near to a system resonance when the response to a stimulus is amplified to a level that will eventually saturate the input of the measurement instrument.

Such saturation for a given range of the input reading of the instrumentation would then be indicative of the onset of impedance unboundedness.

6.3. Data representation and analysis

The Nyquist plot ([2]) is the most common graphical representation of measured complex impedance spectra (Figure 1).

It is a chart where the (negative) imaginary impedance part (reactance),

$$Z_{IM}(f) = \frac{Z(f) - Z^*(f)}{2i}$$

is plotted versus the real impedance part (resistance) [7],

$$Z_{RE} = \frac{Z(f) - Z^*(f)}{2}$$

where $Z(f) = Z_{RE}(f) + i\,Z_{IM}(f)$ and $Z^*(f) = Z_{RE}(f) - i\,Z_{IM}(f)$with $Z(-f) = Z^*(f)$, $\forall f \in \mathbb{R}$,([3]) Z_{RE}, $Z_{IM} \in \mathbb{R}$ and $(\pm i)^2 = -1$.

([2]) Sometimes also called the Cole-Cole plot.
([3]) Superscript * denotes complex conjugation.

It should be noted that the real impedance part is linked to the imaginary impedance part and vice versa by KK principal value (PV) integrals [16,17]:

$$Z_{RE}(\omega) - Z_{\infty} = 2PV \int_0^{\infty} w \frac{Z_{IM}(w)}{\omega^2 - w^2} \frac{dw}{\pi}, \quad \frac{|w|}{w} = \frac{\omega}{|\omega|}, \tag{3}$$

$$Z_{IM}(\omega) = -2PV \int_0^{\infty} \omega \frac{Z_{RE}(w) - Z_{\infty}}{\omega^2 - w^2} \frac{dw}{\pi}, \quad \forall \omega \in \mathbb{R} \tag{4}$$

with $|Z_{\infty}| = \lim_{\omega \to \infty} |Z_{RE}(\omega)| < \infty$ and angular perturbation frequency, $\omega = 2\pi f$ while noting $PV \int_0^{\infty} \frac{dw}{\omega^2 - w^2} = 0$.

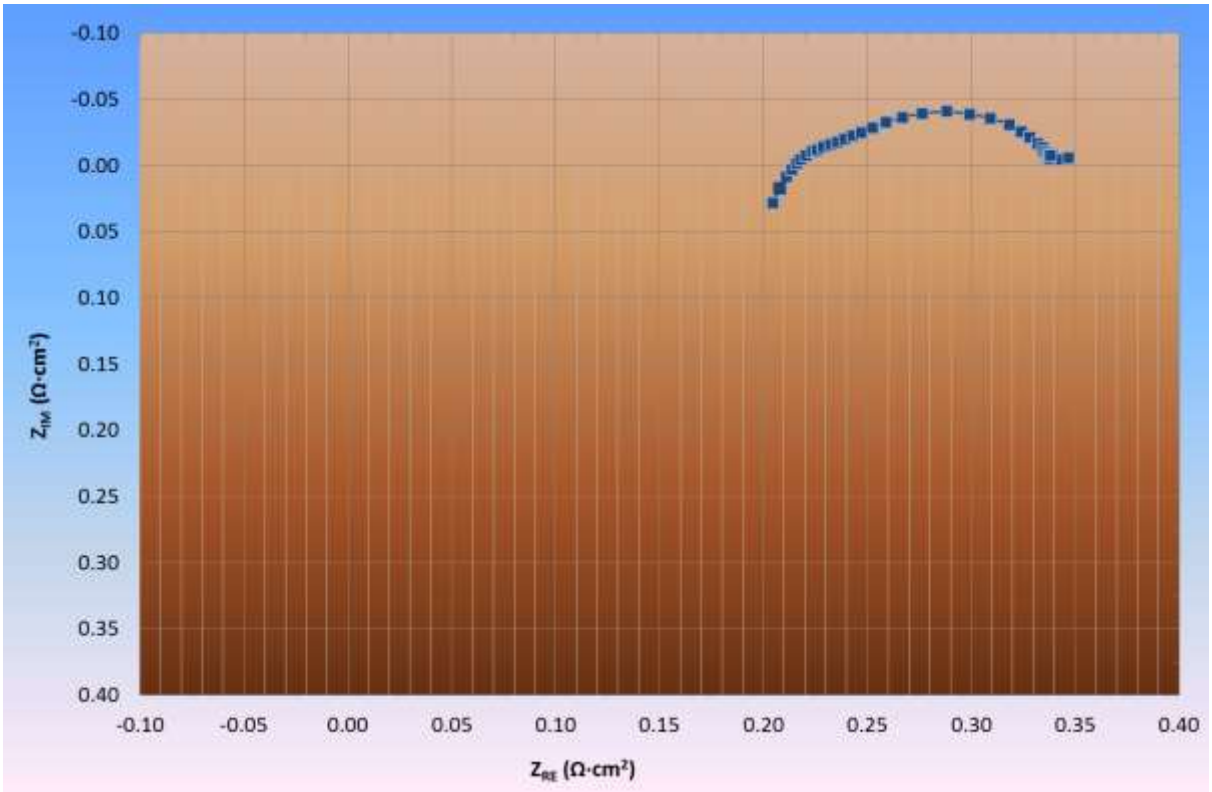

Figure 1 Example of a Nyquist plot for an EIS measurement of a PEMWE cell

The pair of relations (3) and (4) are also known as linear dispersion relations [1-4] for non-singular complex valued quantities.

Such plots usually consist of two or more (depressed ([4])) semicircles representing different electrochemical and transport processes taking place in the PEMWE such as charge transfer, electronic and ionic (proton) conduction in the electrodes, current collectors, electrolyte membrane and wires, convection and diffusion of the reactants and electrode reactions at the active sites on the catalyst.

Note that low impedance devices such as WE cells, often exhibit inductance at high frequencies, mainly due to the cables used in the measurement process. They also exhibit a noisy response at low frequencies.

([4]) A depressed semicircle has its centre below the real axis in a Nyquist plot having the same scale on the abscissa axis and the ordinate axis.

Another graphical representation of recorded EIS data is the Bode plot (Figure 2), which is composed of two individual charts, often combined. One chart plots the impedance magnitude (modulus),

$$|Z(f)| = \sqrt{Z_{RE}^2(f) + Z_{IM}^2(f)}$$

versus the (logarithmic) perturbation frequency, *f*. The other chart plots the impedance phase (principal argument),

$$\theta(f) = \arctan\left(\frac{Z_{IM}(f)}{Z_{RE}(f)}\right), \qquad -\pi \leq \theta < \pi$$

versus the (logarithmic) perturbation frequency, *f*.

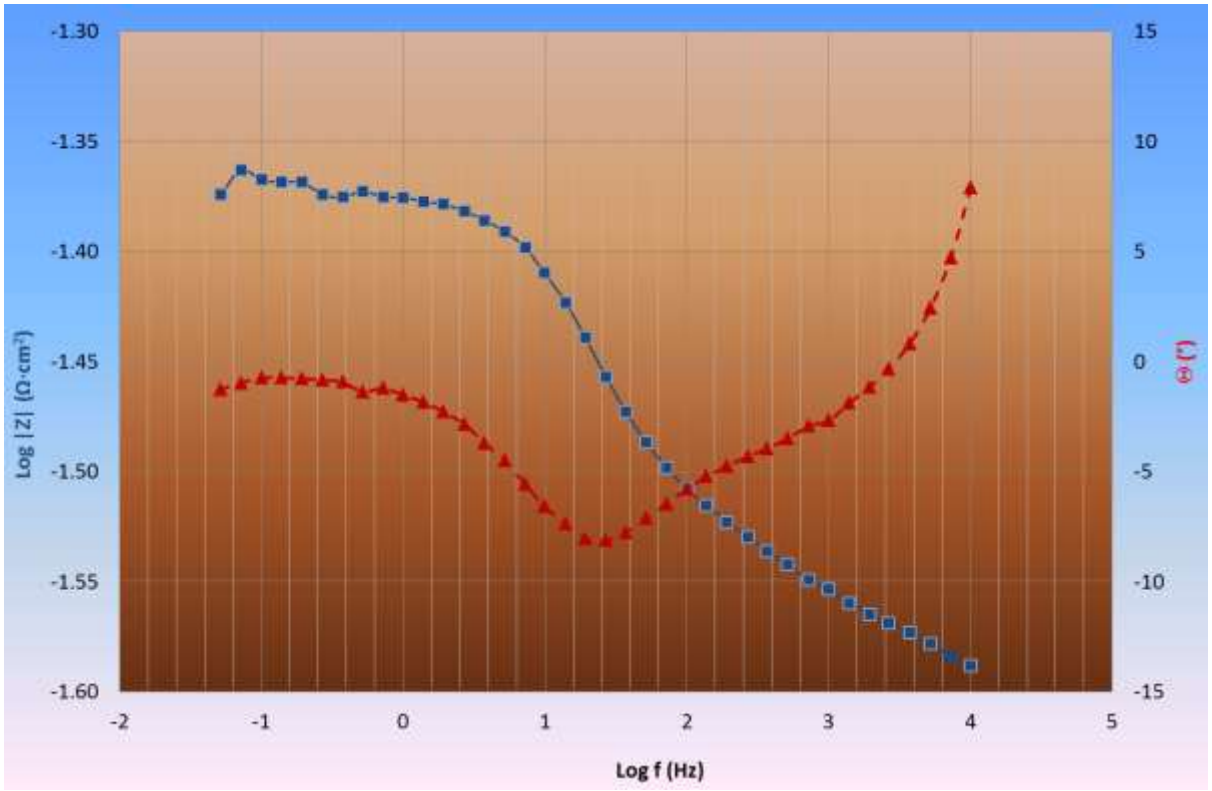

Figure 2 Example of a Bode plot for the EIS data in Figure 1

Similar to the linking of the real and imaginary impedance parts in equations (3) and (4), magnitude and phase are also principally related via principal value integrals known as Bode or gain-phase relations [1-4]. In this case, the natural logarithm is shown on the right hand side of equation (1).

$Z_{RE}(f)$ and $Z_{IM}(f)$ versus the (logarithmic) perturbation frequency, *f*, may also be graphed as a Bode plot, while $\theta(f)$ versus $\ln|Z(f)|$ may be graphed as a Nyquist plot to represent the imaginary part and the real part, respectively.

Furthermore, Nyquist and Bode plots may also be graphed for the admittance, Y (see equation (2)).

The Bode plot can be used to extract information that cannot be readily obtained from Nyquist plots, such as the apparent high and low frequency impedances [1].

In addition, discontinuities and unboundedness in the impedance response may be identified more readily in Bode plots.

In a Nyquist plot, R_Ω is taken as the high frequency, f_{HI} intercept of the arc of the measured impedance on the Z_{RE} axis. R_p is the difference to R_Ω of the total measured impedance taken as the low frequency, f_{LOW} intercept of the arc of the measured impedance with the Z_{RE} axis (see Figure 1).

These are the limits of the real impedance part respectively at high perturbation frequency,

$$\lim_{|f|\to f_{HI}} Z_{IM}(f) = 0$$

and at low perturbation frequency (Figure 1),

$$\lim_{|f|\to f_{LOW}} Z_{IM}(f) = 0$$

and may approximately be determined at zero phase (Figure 2),

$$\lim_{|f|\to f_{LOW}} \theta(f) = \lim_{|f|\to f_{HI}} \theta(f) = 0\,.$$

Plots of impedances versus a power of frequency, or at other levels of immittance (e.g., complex reactance ([5])) may also be used to assist in the further identification of relevant electrochemical and transport processes, particularly diffusion and reaction-related phenomena in the WE cell and to determine suitable initial values for CNLS analysis of EEC fitting the measured data [1-4] ([6]).

Note that, prior to any CNLS analysis, numerical inversion of the recorded frequency domain data into the time domain by a suitable EEC model, known as distribution of relaxation times (DRT) is recommended in order to assist identification of the minimum number of time constants, τ , associated with the electrochemical and transport processes taking place in the WE cell during the EIS measurement [1]. Time constants are, for example, $\tau = \mathrm{RC}$, $\tau = \frac{\mathrm{L}}{\mathrm{R}}$ & $\tau = \sqrt{\mathrm{LC}}$ where R,C and L stand, respectively, for resistance, capacitance and inductance.

Once the number of time constants is known a suitable EEC model that accounts for **all** estimated time constants is to be constructed using a priori knowledge of the physicochemical behaviour of the WE cell tested during the test set-up employed, and a priori knowledge of the operating and test conditions during the EIS measurement.

The EEC model typically comprises various passive elements([7]) (capacitor, inductor and resistor) and distributed elements([8]) (i.e. Gerischer, Nernst, Warburg, etc.) [1-4], combined

([5]) *Immittance* is the general term for these interrelated complex valued quantities [1-4]. It combines the word *im*pedance and ad*mittance* (Henrik Wade Bode).

([6]) For fitting, software is available: LEVM (downloadable at http://jrossmacdonald.com/levmlevmw), EQUIVCRT (downloadable at https://www.utwente.nl/en/tnw/ims/publications/downloads), ZView/Zplot (downloadable at http://www.scribner.com/software), EisPy (downloadable at https://goo.gl/5j7VWM), EIS Spectrum Analyser (http://www.abc.chemistry.bsu.by/vi/analyser), Elchemea Analytical (downloadable at https://www.elchemea.dk) and MEISP (downloadable at http://impedance0.tripod.com) as well as Lin KK Tool (downloadable at https://www.iam.kit.edu/wet/english/Lin-KK.php) for KK testing.

([7]) Passive or lumped elements do not exhibit frequency dispersion. In the time domain, they are represented by ordinary differential equations of integer order of voltage and current.

either in series or in parallel to simulate as closely as possible the impedance of the different components of the WE cell test set-up during the EIS measurement [20,21].

Usually, R_Ω represents the resistance of the electrolyte membrane and of the various conductors used in the test set-up of the WE cell and is modelled as an ideal resistor in series with an ideal inductor, L_c, accounting for the inductance of cables/wires used.

In the simplest case, the interface at each of the two electrodes is modelled by an ideal capacitor representing the double layer charging at the respective electrode interface,

$$C_{dl} = \varepsilon_o \varepsilon_r \frac{A}{\mathrm{d}}$$

in parallel with an ideal resistor accounting for R_p, and specifically the charge-transfer resistance (Figure 3),

$$R_{ct} = \frac{N_A k T}{n_e \mathrm{F} i_0}$$

where ε_o is the permittivity of vacuum (free space), ε_r is the dielectric constant of the electrode, A is its surface area, d is its thickness, N_A is Avogadro's constant, n_e is the number of electrons exchanged in the cell reaction, F is Faraday's constant and i_0 is the exchange current density.

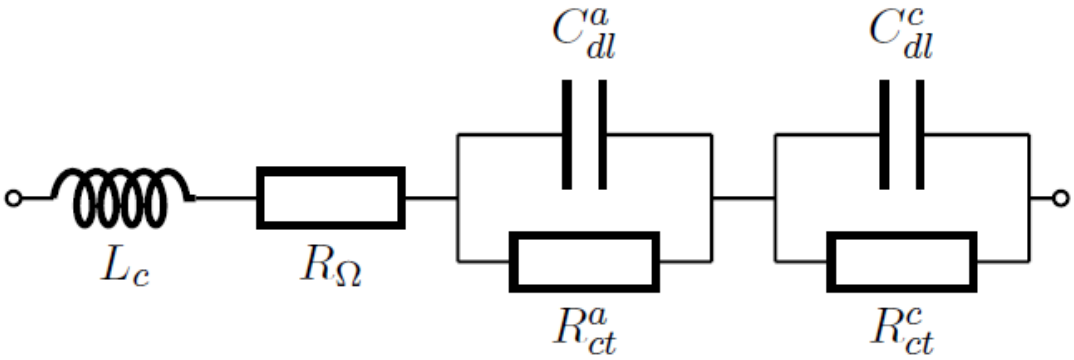

Figure 3 Example of a simple EEC model to simulate that of a PEMWE test set-up accounting for cable/wire inductance, L_c, Ohmic resistance, R_Ω, and two electrodes ([9]) each with double layer capacitance, C_{dl}, and charge transfer resistance, R_{ct}.

More elaborate models may, for example, use a constant phase element (CPE), C_{CPE},([10]) instead of a capacitor to simulate the fractal and porous nature of the electrodes including roughness [34-40], and add a diffusion impedance element, Z_D [42], to account for the species (reactants and water) transport in the respective layers of the electrode, particularly

([8]) Distributed elements (DE) exhibit frequency dispersions and are conventionally expressed by elementary or special functions obtained under simplified assumptions through analytical modelling of partial differential equations of arbitrary order of the perturbed species participating in the mass transfer within the WE cell.

([9]) Anode and cathode are denoted, respectively, by superscripts, ^{a} and ^{c}.

([10]) A CPE has impedance, $Z_{CPE}(\omega)=(Q\ (i\omega))^{-\alpha}$ respectively admittance, $Y_{CPE}(\omega)=Q\ (i\omega)^{\alpha}$ which can be viewed as an imperfect capacitor, $Q=Q_C$ and $0<\alpha\leq 1$, an imperfect inductor, $Q=Q_L$ and $-1\leq\alpha<0$, or an imperfect resistor, $Q=Q_R$ and $0<|i\alpha|\leq 1$ exhibiting dispersion in the frequency domain owing to ordinary time derivatives of non-integer order of voltage and current.

where there is diffusion and/or cell reaction at the catalyst sites, and add, in parallel another series combination of an ideal resistor, R_{ad}, and an ideal inductor, L_{ad}, to account for the dynamics of species adsorption/desorption on the active sites of electrode on the catalyst surfaces.

Sometimes it may be more appropriate to use circuit models assuming ladder structures to simulate the impedance of the WE cell test set-up.

Also, transmission line models (TLM) are sometimes used to supplement EEC models, particularly to simulate the reaction impedance in porous electrode structures, such as the catalyst layer comprising ionic phases (electrolyte with dissolved oxygen) and an electronic phase (metal catalyst on carbon support) and their several interfaces in and along the pores (Figure 4).

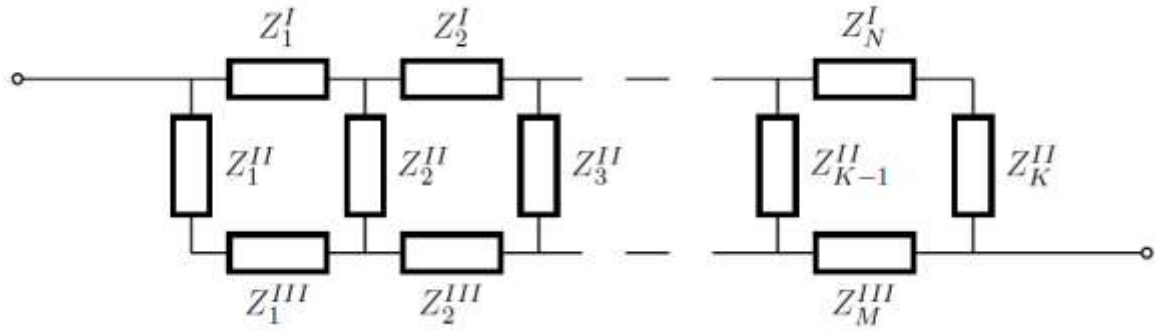

Figure 4 Example of a generic transmission line model with N number of series impedances, Z^I representative of one phase and M number of series impedances, Z^{III} of the same phase arranged in parallel to the former phase and K number of parallel impedances, Z^{II} of another phase.

For example, the series impedances may constitute resistances, $Z^I = R^I$ for the proton-conducting electrolyte phase with dissolved oxygen, and $Z^{III} = R^{III}$ for the electron-conducting phase of the catalyst while the parallel impedances may constitute parallel RC combinations, $Z^{II} = R^{II}(1 + i\omega R^{II} C^{II})$ representing the double-layer capacitance and the charge transfer resistance of the interfaces between the two phases [21-26].

The fitting of impedance data to EEC models and DRT is discussed extensively elsewhere [1-4,17,25-33].

Note that methods other than DRT and CNLS may also be used to analyse the measured data and to extract relevant information [1-4,43].

THIS PAGE IS LEFT BLANK INTENTIONALLY

References

1. E. Barsoukov, J. R. McDonald, Impedance Spectroscopy: Theory, Experiment, and Applications, Third Edition, John Wiley & Sons, Inc., Hoboken, NJ, 2018.
2. A. Lasia, Electrochemical impedance spectroscopy and its applications, Springer, New York, Heidelberg, Dordrecht, London, 2014.
3. V. F. Lvovich, Impedance spectroscopy: applications to electrochemical and dielectric phenomena, John Wiley & Sons, Inc., Hoboken, NJ, 2012.
4. M. E. Orazem, V. Tribollet, Electrochemical impedance spectroscopy, Second Edition, John Wiley & Sons, Inc., Hoboken, NJ, 2017.
5. IEC 62282-7-1 Single Cell Test Methods for Polymer Electrolyte Fuel Cell (PEFC).
6. G. Tsotridis, A. Podias, W. Winkler, M. Scagliotti, The Fuel Cells Testing & Standardisation Network FCTESTNET Fuel Cells Glossary, Office for Official Publications of the European Communities, Luxembourg, June 2006, EUR 22295 EN.
7. ISO 16773-1 Electrochemical Impedance Spectroscopy (EIS) on coated and uncoated specimens. Part. 1. Terms and Definitions.
8. ISO/TR 16208:2014 Corrosion of metals and alloys. Test method for corrosion of materials by electrochemical impedance measurements.
9. Joint Committee for Guides in Metrology, Evaluation of measurement data — An introduction to the Guide to the expression of uncertainty in measurement and related documents, JCGM 104:2009.
10. B. A. Boukamp, Electrochemical impedance spectroscopy in solid state ionics: recent advances, *Solid State Ionics* **169** (2004) 65.
11. M. E. Orazem, B Tribollet, An integrated approach to electrochemical impedance spectroscopy, *Electrochim. Acta* **53** (2008) 7360.
12. B. A. Boukamp, J. R. Macdonald, Alternatives to Kronig-Kramers transformation and testing, and estimation of distributions, *Solid State Ionics* **74** (1994) 85.
13. R. L. de Kronig, On the theory of the dispersion of X-rays, *J Opt Soc Am* **12** (1926) 547.
14. H. A. Kramers, La diffusion de la lumière par les atomes, *Atti. Cong. Intern. Fisica (Trans. Volta Centenary Congr. Como)* **2** (1927) 545.
15. T. Malkow, Immittance Data Validation by Kramers-Kronig Relations – Derivation and Implications, *ChemElectroChem* **4**, 11 (2017) 2777.
16. T. Malkow, G. Papakonstantinou, A. Pilenga, L. Grahl-Madsen, G. Tsotridis, Immittance Data Validation using Fast Fourier Transformation (FFT) Computation – Synthetic and Experimental Examples, *ChemElectroChem* **4**, 11 (2017) 2771.
17. R. A. Latham, Algorithm Development for Electrochemical Impedance Spectroscopy Diagnostics in PEM Fuel Cells, MSc thesis, University of Victoria, Victoria, BC, 2004.
18. R. Makharia, M. F. Mathias, D. R. Baker, Measurement of catalyst layer electrolyte resistance in PEFCs using electrochemical impedance spectroscopy, *J. Electrochem. Soc.* 152, 5 (2005) A970-A977.

19. M. S. Kondratenko, M. O. Gallyamov, A. R. Khokhlov, Performance of high temperature fuel cells with different types of PBI membranes as analysed by impedance spectroscopy, *Int. J. Hydrogen Energy* 37 (2012) 2596-2602.
20. M. Kheirmand, A. Asnafi, Analytic parameter identification of proton exchange membrane fuel cell catalyst layer using electrochemical impedance spectroscopy, *Int. J. Hydrogen Energy* 36 (2011) 13266-13271.
21. S. Cruz-Manzo, R. Chen, A generic electrical circuit for performance analysis of the fuel cell cathode catalyst layer through electrochemical impedance spectroscopy, *J. Electroanal. Chem.* 694 (2013) 45-55.
22. S.-J. Lee, S.-I. Pyun, Effect of annealing temperature on mixed proton transport and charge transfer-controlled oxygen reduction in gas diffusion electrode, *Electrochem. Acta* 52 (2007) 6525-6533.
23. H. Nara, T. Momma, T. Osaka, Impedance analysis of the effect of flooding in the cathode catalyst layer of the polymer electrolyte fuel cell, *Electrochem. Acta* 113 (2013) 720-729.
24. J. R. Macdonald, J. A. Garber, Analysis of Impedance and Admittance Data for Solids and Liquids, *J. Electrochem. Soc.* 124, 7 (1977) 1022-1030.
25. J. R. Macdonald, Three to six ambiguities in immittance spectroscopy data fitting, *J. Phys.: Condens. Matter*, 24 (2012) 175004.
26. J. R. Macdonald, J. Schoonman, A. P. Lehnen, Three dimensional perspective plotting and fitting of immittance data, *Solid State Ionics* 5 (1981) 137-140.
27. J. R. Macdonald Impedance spectroscopy: Models, data fitting, and analysis, *Solid State Ionics* 176, 25–28 (2005) 1961–1969.
28. B. A. Boukamp, A nonlinear lest squares fit procedure for analysis of immittance data of electrochemical systems, *Solid State Ionics* 20 (1986) 31-44.
29. B. A. Boukamp, Impedance Spectroscopy, Strength and Limitations, *Techn. Messen* 71, 9 (2004) 454-459.
30. J. R. Macdonald, L. R. Evangelista, E. Kaminski Lenzi, G. Barbero, Comparison of Impedance Spectroscopy Expressions and Responses of Alternate Anomalous Poisson−Nernst−Planck Diffusion Equations for Finite-Length Situations, *J. Phys. Chem. C* 115, 15 (2011) 7648–7655.
31. J. R. Macdonald, Accelerated Convergence, Divergence, Iteration, Extrapolation and Curve Fitting, *J. Appl. Phys.* 35 (1964) 3034-304.
32. J. R. Macdonald, Fitting Experimental Data, *J. Comp. Phys.* 11 (1973) 620(L).
33. J. R. Macdonald, Limiting electrical response of conductive and dielectric systems, stretched-exponential behavior, and discrimination between fitting models, *J. Appl. Phys.* 82, 8 (1997) 3962-3971.
34. S. Siracusano, V. Baglio, F. Lufrano, P. Staiti, A.S. Aricò, Electrochemical characterization of a PEM water electrolyzer based on a sulfonated polysulfone membrane, J. Mem. Sci. 448 (2013) 209-214.
35. S. Siracusano, S. Trocino, N. Briguglio, V. Baglio, A. S. Aricò, Electrochemical Impedance Spectroscopy as a Diagnostic Tool in Polymer Electrolyte Membrane Electrolysis, Mater. 11, 1368 (2018) 1-15.
36. C. González-Buch, I. Herraiz-Cardona, E. Ortega, J. García-Antón, V. Pérez-Herranz, Study of the catalytic activity of 3D macroporous Ni and NiMo

cathodes for hydrogen production by alkaline water electrolysis, J. Appl. Electrochem. 46 (2016) 791–80.
37. M. Suermann, A. Pătru, T. J. Schmidt, F. N. Büchi, High pressure polymer electrolyte water electrolysis: Test bench development and electrochemical analysis, Int. J. Hydrogen Energy 42 (2017) 12076-12086.
38. I. Dedigama, P. Angeli, K. Ayers, J.B. Robinson, P.R. Shearing, D. Tsaoulidis, D.J.L. Brett, In situ diagnostic techniques for characterisation of polymer electrolyte membrane water electrolysers - Flow visualisation and electrochemical impedance spectroscopy, Int. J. Hydrogen Energy 39 (2014) 4468-4482.
39. J. Polonský, P. Mazúr, M. Paidar, E. Christensen, K. Bouzek, Performance of a PEM water electrolyser using a TaC-supported iridium oxide electrocatalyst Int. J. Hydrogen Energy 39 (2014) 3072-3078.
40. H. Su, V. Linkov, B. J. Bladergroen, Membrane electrode assemblies with low noble metal loadings for hydrogen production from solid polymer electrolyte water electrolysis, Int. J. Hydrogen Energy 38 (2013) 9601-9608.
41. S. H. Frensch, A. C. Olesen, S. S. Araya, S. Knudsen Kær, Model-supported characterization of a PEM water electrolysis cell for the effect of compression, Electrochim. Acta 263 (2018) 228-236.
42. C. Rozain, P. Millet, Electrochemical characterization of Polymer Electrolyte Membrane Water Electrolysis Cells, Electrochim. Acta 131 (2014) 160-167.
43. Z. Stoynov, D. Vladikova, Differential Impedance Analysis, Academic Publishing House Marin Drinov, Sofia, 2005.

THIS PAGE IS LEFT BLANK INTENTIONALLY

GETTING IN TOUCH WITH THE EU

In person

All over the European Union there are hundreds of Europe Direct information centres. You can find the address of the centre nearest you at: https://europa.eu/european-union/contact_en

On the phone or by email

Europe Direct is a service that answers your questions about the European Union. You can contact this service:

- by freephone: 00 800 6 7 8 9 10 11 (certain operators may charge for these calls),

- at the following standard number: +32 22999696, or

- by electronic mail via: http://europa.eu/contact

FINDING INFORMATION ABOUT THE EU

Online

Information about the European Union in all the official languages of the EU is available on the Europa website at: http://europa.eu

EU publications
You can download or order free and priced EU publications from EU Bookshop at: http://bookshop.europa.eu. Multiple copies of free publications may be obtained by contacting Europe Direct or your local information centre (see http://europa.eu/contact).

KJ-NA-29267-EN-C

JRC Mission

As the science and knowledge service of the European Commission, the Joint Research Centre's mission is to support EU policies with independent evidence throughout the whole policy cycle.

EU Science Hub
ec.europa.eu/jrc

@EU_ScienceHub

EU Science Hub - Joint Research Centre

Joint Research Centre

EU Science Hub

Publications Office

doi: 10.2760/67321

ISBN 978-92-79-88738-3